Variable bias current in magnetic bearings for enhanced control system performance and energy efficiency

Ali DIAB*, Armand FARHAT*, Joël MOUTERDE*, and Joaquim DA SILVA*
*Research and Development Department, SKF Magnetics Mechatronics, France
E-mail: ali.diab@skf.com

Abstract
Active Magnetic Bearings (AMBs) offer significant advantages for high-speed and high-precision applications due to their contactless operation, low mechanical wear, and active control capabilities. Conventional control strategies often rely on constant bias currents to linearize the electromagnetic force-current relationship. However, this approach increases energy consumption and introduces non-differentiability in the control inputs, which hinders flatness-based motion planning and reduces overall control performance. This paper proposes a variable bias current allocation strategy formulated as a multi-objective optimization problem. A complementarity function is used to nonlinearly distribute the electromagnetic forces across paired coils, while satisfying physical constraints and reducing energy consumption, without compromising dynamic performance. Experimental validation on an axial AMB test bench demonstrates significant reductions in steady-state power consumption compared to existing approaches. Beyond local performance gains, the proposed strategy ensures a continuous and differentiable force-current relationship. This regularity is essential for integration into a global control architecture combining flatness-based control, state observation, and trajectory planning. This architecture allows further enhancement of system dynamics through accurate trajectory tracking and robust disturbance rejection. The results highlight the dual benefit of the proposed approach: improved energy efficiency and compatibility with advanced AMB control frameworks, grounded in system physics rather than empirical tuning.

Keywords: Optimal bias current, Complementarity function, AMB dynamics performance, AMB energy efficiency, Reference trajectory tracking.

1. Introduction

Active Magnetic Bearings (AMBs) are an advanced alternative to traditional mechanical bearings, offering several advantages such as contactless operation, reduced friction, no need for lubrification, and significantly lower mechanical wear. These features make AMBs highly suitable for demanding applications including aerospace turbines, vacuum pumps, flywheel energy storage systems, and high-speed industrial compressors, where reliability, cleanliness, and longevity are critical.

Despite their benefits, AMBs are inherently energy-intensive due to the continuous power supply required to maintain rotor levitation. The electromagnetic actuators must always remain active, leading to ohmic losses in the stator windings and generating unwanted rotor heating. These power losses are primarily associated with the bias currents needed to ensure system controllability across its operating range (Hu et al., 2004). In conventional control approaches, a constant bias current is applied to each actuator to linearize the coil current and magnetic force relationship. While this simplifies control system design and avoids force-generation dead zones, it also leads to excessive power consumption, particularly in low-load or steady-state operating conditions.

In this context, several control strategies have been developed over the past two decades to improve energy efficiency and robustness of AMB systems. Sliding mode control (Chen and Lin, 2010) and H-infinity control (Cole et al., 2017) have been employed to enhance disturbance rejection and robustness under model uncertainties. Flatness-based nonlinear control methods (Levine et al., 1996) provide systematic tools for reference trajectory generation and tracking, while also

introducing a smooth complementarity function to ensure voltage saturation in an AMB during trajectory planning. Meanwhile, zero-bias and low-bias control schemes (Tsiotras and Wilson, 2004) have been explored to reduce energy losses, although these strategies often introduce control challenges such as instability near zero current and degraded performance in transient regimes. More recent research examined variable bias current scheduling based on load estimation (Yao et al., 2022). Deep reinforcement learning has also been applied to adapt bias currents dynamically under varying operating conditions (Yan et al., 2023). While these approaches offer promising results, they often suffer from a lack of analytical guarantees, require large training datasets, or involve high implementation complexity, which can limit their applicability in safety-critical or industrial environments.

To address the limitations of these existing techniques, this paper proposes an optimal variable bias current strategy, framed as a multi-objective optimization problem. The goal is to define the force-current mapping through two nonlinear complementarity functions that allocate the electromagnetic force across the actuator pair, which can be grounded in system physics. The proposed formulation explicitly incorporates performance and energy efficiency criteria into the design process. Unlike constant bias current schemes, the proposed method dynamically adapts the current distribution according to the desired force command and operating state, thereby reducing power consumption without compromising control performance. The first selected control objective is to ensure accurate tracking of a prescribed force or position trajectory, which is crucial for maintaining precise rotor positioning and stability. The second objective focuses on minimizing energy usage, particularly by reducing the steady-state current and limiting abrupt variations in actuator inputs, which contribute to power loss and thermal stress. By satisfying these competing goals through an optimization-based approach, the controller achieves a favorable balance between performance and efficiency.

The paper is organized as follows. Section 2 outlines the mathematical model of an AMB system and presents two examples of complementarity function. Section 3 introduces the proposed variable bias current strategy, formulated as a multi-objective optimization problem. Section 4 illustrates the control architecture of an active magnetic bearing system with motion planning. Section 5 describes the experimental setup and evaluates the performance of the proposed method in comparison with a reference approach. Finally, Section 5 summarizes the results and conclusions.

2. Problem statement

This section introduces an illustrative model of a one-degree-of-freedom active magnetic bearing and highlights the essential components of its control architecture. The magnetic bearings employs pairs of electromagnets to control motion along a single axis. Since each electromagnet can only exert an attractive force, directly related to the current flowing through its coil, they are arranged in opposing pairs to enable bidirectional force generation.

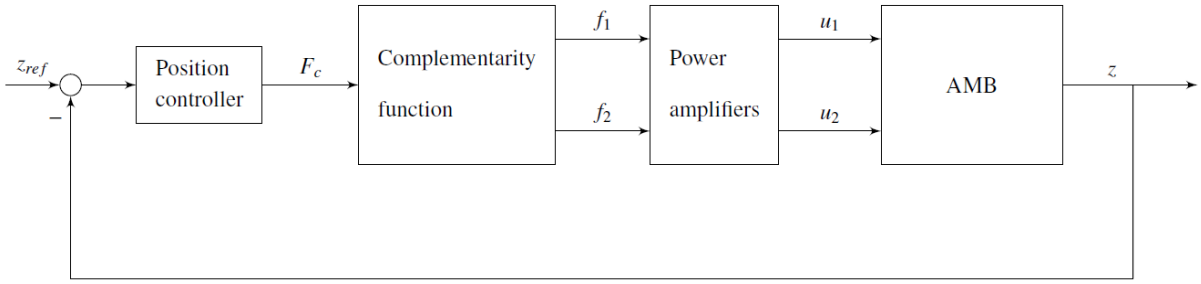

Fig. 1 Block diagram of a closed-loop active magnetic bearing system.

A closed-loop active magnetic bearing system, as depicted in the block diagram of Fig. 1, utilizes a complementarity function to determine the appropriate current distribution between the two electromagnetic coils. The rotor dynamics follow Newton's second law

$$m\ddot{z}(t) = F_1(t) - F_2(t) \tag{1}$$

where z is the rotor position and m is the rotor mass. The attractive force generated by each electromagnet is given by

$$F_j(t) = \kappa i_j^2(t), \quad j \in \{1,2\} \tag{2}$$

assuming a constant scalar κ for simplicity. The currents i_1 and i_2 are governed by the electrical equations

$$u_j(t) = R_j i_j(t) + L_j \frac{di_j(t)}{dt}, \quad j \in \{1,2\} \tag{3}$$

where u_j representing the input voltages and R_j, L_j denoting the resistances and inductances of the circuit, respectively.

The mathematical modeling in this study is simplified to an AMB system with two opposing electromagnets, capturing the system nonlinear force-current characteristics and electrical dynamics using standard formulations. To maintain focus on the fundamental electromechanical and control aspects, the inductance is assumed to be constant, and eddy current effects are neglected. Although such effects can introduce damping and phase lag in some applications, potentially impacting rotor dynamics and control precision, they are omitted here to streamline the analysis. Moreover, the magnetic flux is not explicitly addressed, as it is considered directly proportional to the current through the constant inductance in this simplified case.

Due to the nonlinear dependence of force on current, controlling the system is challenging. Indeed, a pair of nonlinear complementarity functions f_1 and f_2 maps the desired force command F_c to reference currents inputs

$$i_1^*(t) = f_1(F_c(t)) \quad \text{and} \quad i_2^*(t) = f_2(F_c(t)) \tag{4}$$

These functions are designed to allocate the force between the two actuators in a way that enhances control performance. In the following of this section, we present two examples of complementarity functions largely used in the literature.

First, consider the case of constant bias current. In this case, the complementarity functions f_1 and f_2 are respectively defined as

$$f_{10}(F_c) = \begin{cases} i_0 + \Delta i(F_c) & if\ -i_0 < \Delta i(F_c) \\ 0 & otherwise \end{cases} \quad \text{and} \quad f_{20}(F_c) = \begin{cases} i_0 - \Delta i(F_c) & if\ \Delta i(F_c) < i_0 \\ 0 & otherwise \end{cases}$$

where i_0 is a constant bias current and Δi is defined as

$$\Delta i(F_c) = \begin{cases} i_0 - \sqrt{\dfrac{-F_c}{\kappa}} & if\ \mathrm{F_c} < -4\kappa i_0^2 \\ \dfrac{F_c}{4\kappa i_0} & if\ -4\kappa i_0^2 \le \mathrm{F_c} \le 4\kappa i_0^2 \\ -i_0 + \sqrt{\dfrac{F_c}{\kappa}} & if\ 4\kappa i_0^2 < \mathrm{F_c} \end{cases} \tag{5}$$

Since system (1)-(3) is differentially flat (Levine et al., 1996), given an imposed reference force trajectories F_c and following the above constant bias complementarity function (4)-(5), the input voltages can be expressed as

$$u_1(t) = \begin{cases} 0 & if\ \mathrm{F_c}(t) < -4\kappa i_0^2 \\ R_1 i_0 + \dfrac{R_1 F_c(t)}{4\kappa i_0} + \dfrac{L_1 \dot{F}_c(t)}{4\kappa i_0} & if\ -4\kappa i_0^2 \le \mathrm{F_c}(t) \le 4\kappa i_0^2 \\ R_1 \sqrt{\dfrac{F_c(t)}{\kappa}} + \dfrac{L_1 \dot{F}_c(t)}{2\sqrt{\kappa F_c(t)}} & if\ 4\kappa i_0^2 < \mathrm{F_c}(t) \end{cases}$$

and

$$u_2(t) = \begin{cases} R_2 \sqrt{\dfrac{-F_c(t)}{\kappa}} - \dfrac{L_2 \dot{F}_c(t)}{2\sqrt{-\kappa F_c(t)}} & if\ \mathrm{F_c}(t) < -4\kappa i_0^2 \\ R_2 i_0 - \dfrac{R_2 F_c(t)}{4\kappa i_0} - \dfrac{L_2 \dot{F}_c(t)}{4\kappa i_0} & if\ -4\kappa i_0^2 \le \mathrm{F_c}(t) \le 4\kappa i_0^2 \\ 0 & if\ 4\kappa i_0^2 < \mathrm{F_c}(t) \end{cases}$$

where $\dot{F}_c$ is the time derivative of the imposed reference force trajectory.

Conventional linear control approaches typically employ constant bias currents to linearize the force-current relationship and to avoid singularities at zero force command $F_c = 0$. Increasing the bias current avoids singularity but

amplifies electromagnetic losses, which are related to iron losses and rotor heating. In some industrial applications such as vacuum pumps, where the rotor heat cannot be easily evacuated, the possibility of avoiding biasing currents without penalizing the dynamical requirements of the bearings is of particular interest. Additionally, the derived expressions for the voltage inputs u_1 and u_2 exhibit non-differentiability at $F_c = -4\kappa i_0^2$ and $F_c = 4\kappa i_0^2$, respectively, which complicates the motion planning problem that requires smooth reference trajectories.

To overcome this, (Levine et al., 1996) proposed using smooth, differentiable polynomial-based complementarity function given by

$$f_{1\eta}(F_c) = \begin{cases} 0 & if\ F_c < -\eta \\ \frac{P_\eta(F_c)}{\sqrt{\kappa}} & if\ -\eta \le F_c \le \eta \\ \sqrt{\frac{F_c}{\kappa}} & if\ F_c > \eta \end{cases} \quad \text{and} \quad f_{2\eta}(F_c) = \begin{cases} \sqrt{\frac{-F_c}{\kappa}} & if\ F_c < -\eta \\ \sqrt{\frac{P_\eta^2(F_c) - F_c}{\kappa}} & if\ -\eta \le F_c \le \eta \\ 0 & if\ F_c > \eta \end{cases} \tag{6}$$

where η is a positive constant scalar and the polynomial P_η is given by

$$P_\eta(F_c) = \frac{15}{16}\eta^{-\frac{5}{2}}(F_c+\eta)^3 - \frac{13}{16}\eta^{-\frac{7}{2}}(F_c+\eta)^4 + \frac{17}{64}\eta^{-\frac{9}{2}}(F_c+\eta)^5 - \frac{1}{32}\eta^{-\frac{11}{2}}(F_c+\eta)^6$$

This polynomial-based complementarity function leads to smoother voltage profiles and enables motion planning and continuous reference trajectory tracking.

3. Optimal bias current

This section shows that the complementarity function can be derived as the solution of a multi-objective optimization problem. In this paper, we focus on the following two criteria:

1- Accurate tracking of a desired reference trajectory.

2- Enhanced system dynamics with minimized power consumption.

To achieve accurate trajectory tracking, the total generated electromagnetic force, $F_1 - F_2$, must match the reference force command F_c, meaning that $F_c = F_1 - F_2$. Using (1) and (2), this requirement leads to

$$f_1^2(F_c) - f_2^2(F_c) = F_c/\kappa \tag{7}$$

This constraint, derived from Criterion 1, ensures that the complementarity function enforces input-output linearization of the active magnetic bearing system, enabling control design based on system inversion and able to follow an imposed reference trajectory (Levine et al., 1996). Consequently, the problem is reduced to designing a suitable function f_1 through a multi-objective optimization problem. Once f_1 is determined, the corresponding f_2 is directly obtained using (7).

In this paper, the selected cost function balances between improving dynamic performance and reducing energy usage. The steady-state energy consumption is approximated by the sum of squared coil currents, while the dynamic behavior of the system is related to the rate of change of electromagnetic forces, dF_j/dt. However, the dynamic response can be characterized primarily by variations in electromagnetic force with respect to current, dF_j/di_j, assuming fast current control dynamics.

Therefore, based on these considerations, the proposed optimization problem can be formulated as

$$\text{Minimize}\ \ i_1^2 + i_2^2 + \frac{\alpha}{\left|\frac{dF_1}{di_1}\right| + \left|\frac{dF_2}{di_2}\right|} \tag{8}$$

A large weighting factor α can improve dynamic performance at the expense of higher power consumption. Moreover, a variable α can be used to satisfy some physical constraints.

Fig. 2 compares different complementarity functions in the normalized coordinates. The constant bias complementarity function is linear inside the interval $[-0.64,\ 0.64]$ and it is not differentiable at $F_c = \pm 0.64$. The polynomial complementarity function $f_{1\eta}$ is differentiable. The proposed optimal complementarity function f_{1op} set the minimal current command around an operating condition to minimize power consumption.

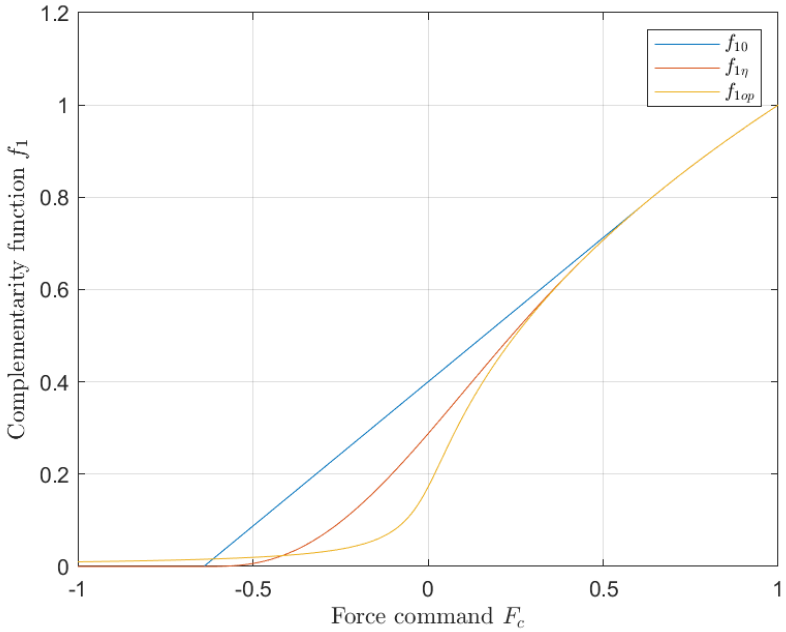

Fig. 2 Normalized complementarity functions: Constant bias complementarity function f_{10}; Polynomial complementarity function $f_{1\eta}$ given in (6); Proposed optimal complementarity function f_{1op}.

4. Control architecture with motion planning

This section presents the developed control architecture for active magnetic bearing systems, that integrates motion planning techniques to enhance rotor positioning performance. By combining reference trajectory generation with bias current modulation, the system aims to ensure dynamic efficiency while respecting constraints such as voltage and current saturation.

As illustrated in Fig. 3, the proposed AMB control architecture consists of the following interconnected components:

- Reference trajectory generator: Computes the desired rotor position z_{ref} and the associated reference force F_{ref}, based on the system objectives and motion planning requirements.
- Position controller: Computes the required force command F_c that drives the rotor toward the target based on the reference and actual rotor position, while compensating for dynamic deviations and disturbances.
- Complementarity function: Translates the force command F_c into reference currents i_1^* and i_2^*. This function ensures a differentiable force-current relationship, allowing accurate and energy-efficient current distribution between actuator coils.
- Current controllers: Regulate the actual coil currents by adjusting the input voltages u_1 and u_2, compensating for coil resistance and inductance to ensure accurate tracking of the current references.
- Magnetic and mechanical observers: These observers are based on a physical model of the AMB system that has inputs the measured position, currents, and voltages, to estimate internal states. These include electromagnetic forces, rotor velocity, and external disturbance forces.

The use of smooth, differentiable complementarity functions enables compatibility with trajectory generation methods (Xia et al., 2021), avoids control singularities, and reduces steady-state power losses associated with constant bias strategies.

The proposed architecture supports magnetic forces and mechanical disturbances estimation, enabling advanced functionalities such as disturbance rejection and fault detection. It also ensures compliance with system constraints, including current and voltage saturation, which is critical in safety-critical applications.

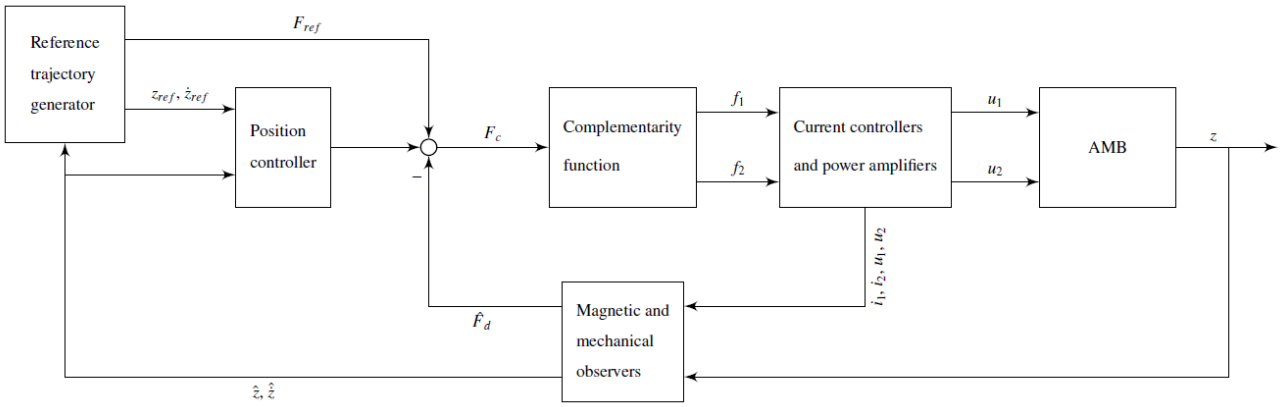

Fig. 3 Block diagram of the proposed AMB control architecture integrating motion planning.

This paper focuses on the design of the complementarity function. The reference trajectory generation and the magnetic force estimation algorithm are based on existing physical modeling techniques and are not detailed in this work.

5. Experimental results

To assess the effectiveness of the proposed control method, experimental tests were carried out on an axial active magnetic bearing test bench. The AMB setup is equipped with position sensors, current and voltage measurement, and real-time control. Due to the use of non-laminated materials, the system exhibits non-negligible eddy current effects that influence the system dynamic behavior. While specific design parameters are not detailed, the test bench reflects key characteristics of industrial AMB systems and provides a representative platform for evaluating the proposed control strategy.

Two experimental tests were carried out. In the first test, we compare between the polynomial complementarity function given in (6) and the proposed optimal complementarity function. To assess the dynamic performance of the AMB system associated with a given complementarity function, a step reference position is applied. Therefore, the dynamic performance is evaluated at the transient phase and the energy consumption performance is evaluated at steady state. In the second test, the motion planning control architecture proposed in Section 4 is tested to disturbance rejection.

5.1. Performance comparison of the polynomial and optimal complementarity functions

In this test, the proposed optimal complementarity function is compared with the polynomial complementarity function in (6). The rotor position responses were recorded under no-load levitation conditions ($F_d = 0$) and compared for two settings: one employing the polynomial complementarity function defined in (6), and another using the proposed optimal strategy.

The position controller used for both settings was a classical proportional-integral-derivative (PID) controller. Fig. 4 presents the corresponding rotor position responses in the normalized coordinates under the same PID tuning parameters. For $t < 0.4$ seconds, the current references are arbitrary set to bring the rotor into contact with the auxiliary mechanical bearings. At $t = 0.4$ seconds, a levitation order is applied. As shown in this figure, the proposed optimal strategy leads to a notable reduction in rotor overshoot and a faster transient response. At steady-state, the measured currents are lower using the optimal complementarity function, an important metric since power consumption is proportional to the square of the coil current. These outcomes confirm that the variable bias current approach significantly enhances both control performance and energy efficiency.

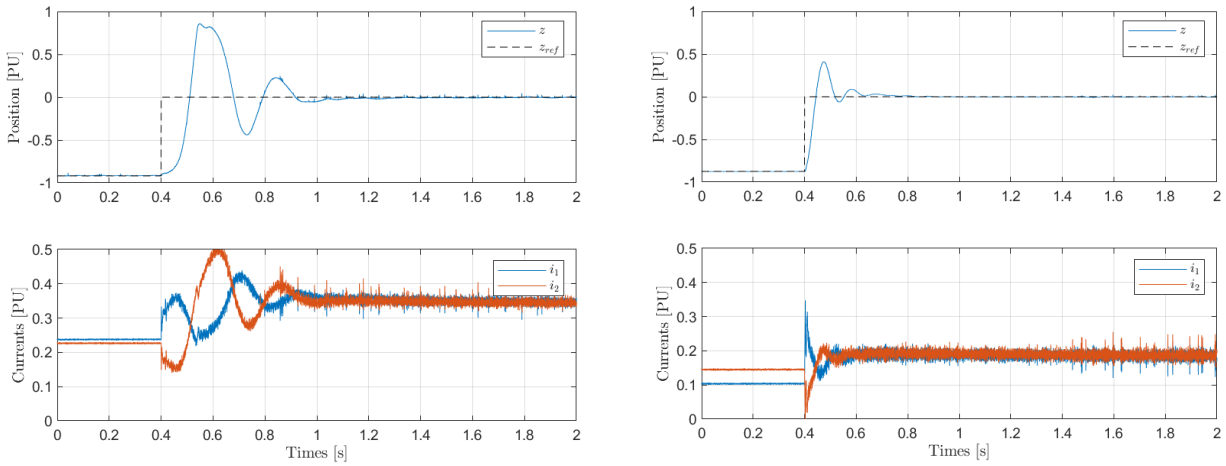

Fig. 4 Comparison of the rotor responses in a levitation scenario, shown in normalized coordinates: (left) with the polynomial-based complementarity function from (6); (right) with the proposed optimal complementarity function.

5.2. Disturbance rejection performance of the proposed control architecture

This section validates the robustness of the proposed control framework under external disturbance conditions. The experimental setup incorporates a secondary axial active magnetic bearing (AMB), which is used to apply a disturbance force to the rotor, while the primary AMB actively compensates for it to maintain rotor stability.

Two control approaches are compared:

1- Conventional PID control: A classical PID position controller with constant bias current, operating without any reference trajectory generation.

2- Proposed control architecture: The complete control scheme presented in Section 4, incorporating reference trajectory generation, the optimized complementarity function for current allocation, and model-based disturbance estimation.

In this experimental test, a sinusoidal disturbance force with an amplitude equal to 50% the primary AMB force capacity and frequency $1\ Hz$ is applied by the secondary AMB. Fig. 5 presents the corresponding results. On the left, using conventional PID control, the rotor displacement remains bounded, but exhibits a high oscillation amplitude. The bottom plot shows the corresponding force command F_c issued by the PID controller. On the right, with the proposed control architecture, the rotor displacement is reduced by approximately 50% compared to the conventional approach, and the rotor follows the computed reference trajectory z_{ref}, which is updated in real time. Furthermore, the proposed control system provides an accurate estimation $\hat{F}_d$ of the applied disturbance force, using a model-based magnetic observer.

To further evaluate the robustness of the proposed control strategy, the experiment was repeated under various disturbance force profiles, including triangular and step disturbance forces. Across all test cases, the proposed control architecture consistently outperformed the conventional PID-based approach by significantly reducing rotor displacement and delivering accurate real-time estimation of the applied disturbance forces. These results demonstrate the adaptability and reliability of the proposed method under dynamic operating conditions, confirming its effectiveness in enhancing disturbance rejection, minimizing rotor deviation, and supporting advanced control functionalities such as force observation and trajectory tracking. As such, the strategy presents a robust and energy-efficient solution for high-performance AMB systems subject to unpredictable external perturbations.

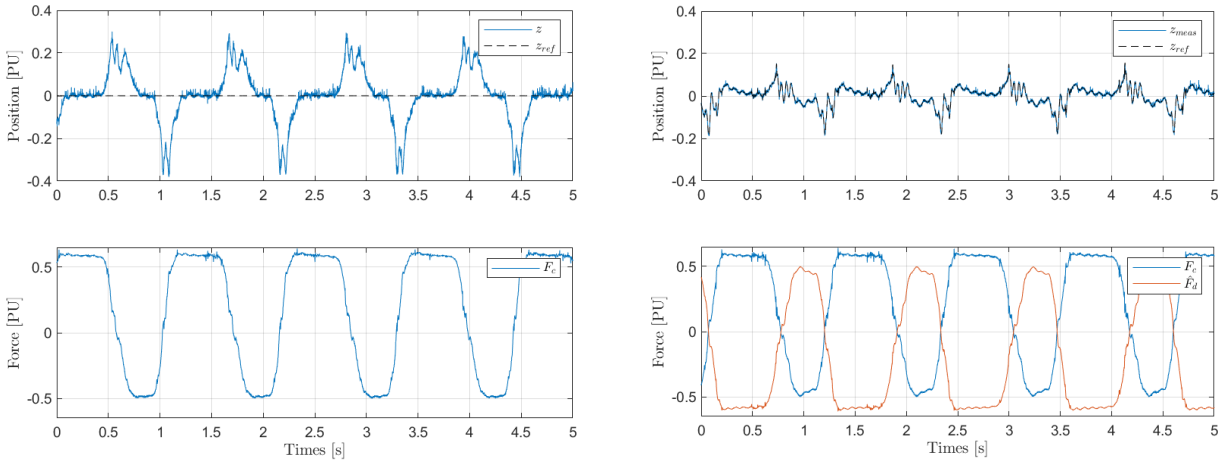

Fig. 5 Rotor response comparison under disturbance rejection in normalized coordinates: (left) using a conventional PID controller without trajectory tracking and using a constant bias current; (right) using the proposed control approach incorporating trajectory generation and the optimized complementarity function.

6. Conclusion

This paper presented a control strategy for active magnetic bearings based on a variable bias current approach, derived from a multi-objective optimization framework. The proposed method introduces nonlinear complementarity functions to distribute electromagnetic forces while balancing two key objectives: precise trajectory tracking and reduced energy consumption. By formulating the bias current as an optimization variable, the strategy enables improved dynamic performance without the excessive power losses typically associated with constant bias schemes. Experimental results obtained from an axial AMB test bench confirmed the effectiveness of the proposed approach, demonstrating faster rotor stabilization, smaller displacements, and lower steady-state energy usage compared to conventional methods. The use of smooth, differentiable functions also facilitates the implementation of advanced control and motion planning techniques. Future work will focus on exploring alternative objective functions and developing advanced nonlinear position controllers and adaptive strategies within this complementarity-based framework.

References

Chen, S. Y. and Lin, F. J., Robust nonsingular terminal sliding-mode control for nonlinear magnetic bearing system, IEEE Transactions on Control Systems Technology, Vol.19, No.3 (2010), pp.636-643.

Cole, M. O., Chamroon, C., and Keogh, P. S., H-infinity controller design for active magnetic bearings considering nonlinear vibrational rotordynamics, Mechanical Engineering Journal, Vol.4, No.5 (2017), pp.16-00716.

Hu, T., Lin, Z., and Allaire, P.E., Reducing power loss in magnetic bearings by optimizing current allocation, IEEE Transactions on Magnetics, Vol.40, No.3 (2004), pp.1625-1635.

Levine, J., Lottin, J., and Ponsart, J. C., A nonlinear approach to the control of magnetic bearings, IEEE Transactions on Control Systems Technology, Vol.4, No.5 (1996), pp.524-544.

Tsiotras, P. and Wilson, B. C., Zero-and low-bias control designs for active magnetic bearings, IEEE Transactions on Control Systems Technology, Vol.11, No.6 (2004), pp.889-904.

Xia, Y., Lin, M., Zhang, J., Fu, M., Li, C., Li, S., and Yang, Y., Trajectory planning and tracking for four-wheel steering vehicle based on differential flatness and active disturbance rejection controller, International Journal of Adaptive Control and Signal Processing, Vol.35, No.11 (2021), pp.2214-2244.

Yang, B., Peng, C., Jiang, F., and Shi, S., A novel model calibration method for active magnetic bearing based on deep reinforcement learning, Guidance, Navigation and Control, Vol.3, No.3 (2023), pp.2350017.

Yao, Y., Ren, G., and Yu, S., Division linearization zero-bias current control for AMBs-rotor system with uncertainties and saturation, IEEE Transactions on Industrial Electronics, Vol.70, No.10 (2022), pp.10557-10566.